Crossover from Fermi Liquid to Wigner Molecule Behavior in Quantum Dots

R. Egger,[1] W. Häusler,[1] C. H. Mak,[2] and H. Grabert[1]

[1]*Fakultät für Physik, Albert-Ludwigs-Universität, D-79104 Freiburg, Germany*
[2]*Department of Chemistry, University of Southern California, Los Angeles, California 90089-0482*
(Received 11 November 1998)

The crossover from weak to strong correlations in parabolic quantum dots at zero magnetic field is studied by numerically exact path-integral Monte Carlo simulations for up to eight electrons. By the use of a multilevel blocking algorithm, the simulations are carried out free of the fermion sign problem. We obtain a universal crossover governed only by the density parameter r_s. For $r_s > r_c$, the data are consistent with a Wigner molecule description, while, for $r_s < r_c$, Fermi liquid behavior is recovered. The crossover value $r_c \approx 4$ is surprisingly small.   [S0031-9007(99)08929-2]

PACS numbers: 73.20.Dx, 71.10.Ay, 71.10.Ca

Quantum dots can be considered as solid-state artificial atoms with tunable properties. Confining a small number of electrons N in a two-dimensional electron gas in semiconductor heterostructures, a number of interesting effects arising from the interplay between confinement and the Coulomb interaction between the electrons can be observed [1,2]. Since the confinement potential is usually quite shallow, the long-ranged Coulomb interaction among the electrons plays a prominent role, and in contrast to conventional atoms effective single-particle approximations quickly become unreliable. In the low-density (strong-interaction) limit, $r_s \to \infty$, classical considerations suggest a Wigner crystal-like phase with electrons spatially arranged in shells [3]. With quantum fluctuations, such a phase is best described as a Wigner molecule. In contrast, for high densities (weak interactions), $r_s \to 0$, a Fermi liquidlike description is expected to be valid, where it is more appropriate to think of the behavior as resulting from the single-particle orbitals being filled. The noninteracting limit [4] is then typically used as a starting point for the theoretical description of quantum dots.

To date, no reliable information exists for the crossover between these two limits. This is mainly due to a complete lack of sufficiently accurate methods that are able to cover the full range of r_s, especially when no magnetic field is present. Exact diagonalization techniques are limited to very small particle numbers and small r_s; otherwise, a large error due to the truncation of the Hilbert space arises [5]. Hartree-Fock calculations become increasingly unreliable for large r_s and are known to incorrectly favor spin-polarized states [6]. Similarly, density functional calculations [7] introduce uncontrolled approximations in the absence of exact reference data. In principle, the quantum Monte Carlo (QMC) method is the best candidate for producing reliable data for quantum dots. Unfortunately, the notorious fermion sign problem makes direct QMC simulations almost impossible [8]. To avoid the sign problem, the fixed-node approximation and a related variational approach have been employed in Ref. [9], but the results are no longer exact.

In this Letter, we adopt a radically different approach to fermion QMC simulations, based on the recently developed multilevel blocking (MLB) algorithm [10,11]. The MLB algorithm is able to provide numerically exact QMC results free of the sign problem. In this Letter, we report large-scale simulation results for the weak-to-strong-correlation crossover for up to eight electrons. The numerical results at large r_s are shown to agree with a Wigner molecule description.

Model.—We study a two-dimensional parabolic quantum dot at zero magnetic field,

$$H = \sum_{j=1}^{N}\left(\frac{p_j^2}{2m^*} + \frac{m^*\omega_0^2}{2}x_j^2\right) + \sum_{i<j=1}^{N}\frac{e^2}{\kappa|x_i - x_j|}, \tag{1}$$

where the positions (momenta) of the electrons are denoted by $x_j (p_j)$. The effective mass is m^*, and the dielectric constant is κ. The MLB calculations are carried out at fixed N and fixed $S = (N_\uparrow - N_\downarrow)/2$, the z component of the total spin. We present results for the energy, $E = \langle H \rangle$, the radial charge and spin densities $\rho(r)$ and $s_z(r)$ normalized to $\int_0^\infty dr\, 2\pi r \rho(r) = N$ and $\int dr\, 2\pi r s_z(r) = S$, and the two-particle correlation function

$$g_S(x) = \frac{2\pi l_0^2}{N(N-1)}\left\langle \sum_{i\neq j=1}^{N}\delta(x - x_i + x_j)\right\rangle. \tag{2}$$

g_S is isotropic, and with $y = r/l_0$ prefactors are chosen such that $\int_0^\infty dy\, y g_S(y) = 1$. The length scale $l_0 = \sqrt{\hbar/m^*\omega_0}$ from the confinement allows the interaction strength to be parametrized by $\lambda = l_0/a = e^2/\kappa\omega_0 l_0$, where a is the effective Bohr radius. For any given N and λ, the dimensionless density parameter r_s can then be obtained from the data, $r_s = r^*/a$, where r^* corresponds to the first maximum in $\sum_S g_S(r)$. The values for r_s obtained this way agree well with the predictions of an electrostatic point-charge model [12]. In all simulations, the temperature was set to $T = 0.1\hbar\omega_0/k_B$.

Method.—The simulation method is based on a standard discretized path-integral representation of the observables of interest, where the sampling is done according to

0031-9007/99/82(16)/3320(4)$15.00

the MLB algorithm described in detail in Ref. [10]. A sample number [10] of at most $K = 600$ was sufficient to eliminate bias from the algorithm, and at the same time cured the sign problem. The simulations have been carried out on up to five levels in the MLB scheme. Data were collected from several 10^4 samples for each parameter set $\{N, S, \lambda\}$, with a typical CPU time requirement of a few days (for each set) on a SGI Octane workstation. As a validation for this procedure, we have accurately reproduced the exact diagonalization results for $N = 2$ electrons [5].

Charge and spin densities.—Figure 1 shows the charge density $\rho(r)$ of the spin-polarized state for $N = 5$ to 8 electrons. While for $\lambda = 2$ increasing N does not change $\rho(r)$ qualitatively, the situation is different for strong interactions ($\lambda = 8$), signifying the onset of shell formation in real space. Such a structure is clear evidence for Wigner molecule behavior. The classical shell filling sequence has been predicted recently [3]. For $N < 6$, there is only one shell, but the sixth electron enters a new inner shell (1-5). Furthermore, for $N = 7$ the shell filling is 1-6, and for $N = 8$ it is 1-7. These predictions are in accordance with our data. Additional simulations for up to 12 electrons at $\lambda = 8$ (not shown here) further verify the classical filling sequence. The only exception is $N = 10$, where we find a 3-7 instead of the predicted 2-8 structure. Clear indications of a spatial shell structure at $N \geq 6$ can be observed even for $\lambda = 4$, albeit significantly less pronounced than for $\lambda = 8$. For $\lambda \gtrsim 4$, the charge densities are found to be quite insensitive to S. This is expected for a Wigner crystal where particle statistics and spin influence energies or density correlations only weakly. Our numerical results for the spin density in this regime simply follow the corresponding charge density according to $s_z(r) \simeq (S/N)\rho(r)$. A significant S dependence of charge and spin densities is observed only for weak correlations.

Crossover.—To quantitatively investigate the crossover from weak to strong correlations, we employ the quantity

$$\xi_N(r_s) \propto \sum_{S,S'} \int_0^\infty dy\, y |g_S(y) - g_{S'}(y)|, \qquad (3)$$

normalized such that in the absence of interactions $\xi_N = 1$. The correlation function $g_S(r)$ in Eq. (2) is a very sensitive measure of Fermi statistics, in particular, revealing the spin-dependent correlation hole. Since interactions tend to destroy the Fermi surface, the spin sensitivity of $g_S(r)$ is largest for a Fermi gas, $r_s = 0$. In fact, for $r_s \to \infty$, the correlation function $g_S(r)$ becomes completely spin independent. Hence the quantity $\xi_N(r_s)$ decays from unity at $r_s = 0$ down to zero as $r_s \to \infty$. The functional form of this decay is indicative of the crossover under consideration.

As seen in Fig. 2, the crossover curve $\xi_N(r_s)$ becomes remarkably *universal* and depends only weakly on N. Its decay defines a crossover scale r_c, where a simple

exponential fit for small r_s yields $r_c \approx 4$. For $r_s > r_c$, the functional form of $\xi(r_s)$ is better described by

$$\xi(r_s) \propto \exp\left(-\sqrt{r_s/r_c'}\right), \qquad (4)$$

where $r_c' \approx 1.2$. We mention in passing that the WKB estimate for $\langle \psi_S | H | \psi_S \rangle - \langle \psi_{S'} | H | \psi_{S'} \rangle$ exhibits the same large-r_s dependence. One can therefore argue that the spin sensitivity of the square of the eigenfunctions $|\psi_S|^2$ also shows this behavior, and thereby rationalize Eq. (4). The value $r_c \approx 4$ is consistent with the appearance of spatial shell structures in the density profile. In addition, the energy spectrum is in accordance with a Wigner molecule description for $r_s > r_c$ (see below). Summarizing, the crossover from weak to strong correlations is characterized by the rather small value $r_c \approx 4$.

Parenthetically, we contrast this result with the values $r_c^{WC} \approx 37$ found for clean [13] and $r_c^{dis} \approx 7.5$ for disordered [14] unbounded systems. The latter result provides evidence that breaking the continuous translation invariance stabilizes the crystallized phase. The even smaller r_c found here should then be due to the confinement. Caution is advised with the thermodynamic limit, $\omega_0 \to 0$ with r_s fixed, where plasmon modes eventually govern the low-energy physics. There the value r_c^{WC} becomes relevant. For GaAs-based structures with $r_s = 4$, we estimate that
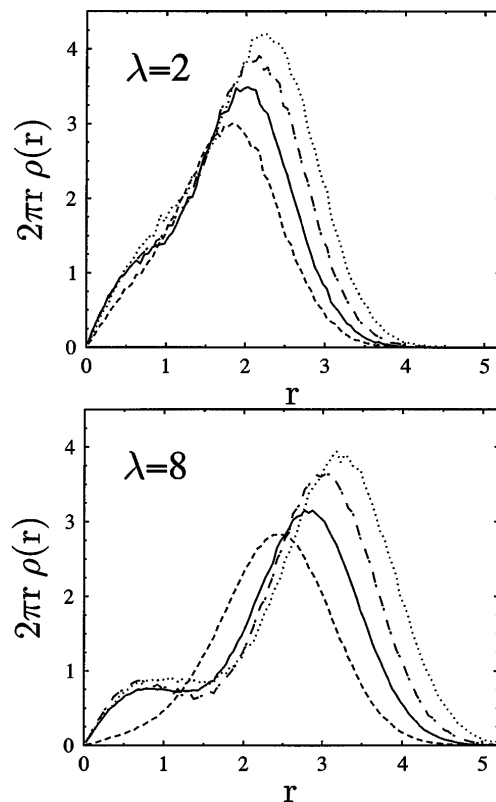

FIG. 1. Density $\rho(r)$ of the spin-polarized state ($S = N/2$) for $\lambda = 2$ (top) and $\lambda = 8$ (bottom). Dashed, solid, dash-dotted, and dotted curves correspond to $N = 5$, 6, 7, and 8, respectively. Units are such that $l_0 = 1$.

spin-sensitive properties lose their significance only for very large electron numbers, $N \gtrsim 10^4$.

Energies.—MLB results for the energy at different parameter sets $\{N, S, \lambda\}$ are listed in Table I. For given N and λ, if the ground state is (partially) spin polarized with spin S, the simulations should yield the same energies for all $S' < S$. Within the accuracy of the calculation, this consistency check is indeed fulfilled.

Detailed data are given in Table I. For $N = 3$ electrons, as r_s is increased, a transition occurs from the $S = 1/2$ to a spin-polarized $S = 3/2$ ground state at an interaction strength $\lambda \approx 5$ corresponding to $r_s \approx 8$. For $N = 4$, we encounter a Hund's rule case. By using perturbation theory in r_s, one may show that the interactions lead to a $S = 1$ ground state. From our data, this standard Hund's rule (which applies for small r_s) is seen to hold throughout the full range of r_s, and the ground state spin stays $S = 1$ even for large r_s. A similar situation arises for $N = 5$ electrons, where the ground state is characterized by $S = 1/2$ for all r_s. Turning to $N = 6$, while one has filled orbitals and hence a zero-spin ground state for weak correlations, our results for $\lambda = 8$ reveal a transition to a $S = 1$ ground state as r_s is increased. A similar transition from a $S = 1/2$ ground state for weak correlations to a partially spin-polarized $S = 5/2$ ground state is found for $N = 7$ electrons. Finally, for $N = 8$, as expected from Hund's rule, a $S = 1$ ground state is observed for small r_s. However, for $\lambda \gtrsim 4$, corresponding to $r_s \gtrsim 10$, the ground state is seen to have spin $S = 2$, in contrast to the conventional Hund's rule prediction.

For strong correlations, $r_s > r_c$, the energy levels and their spin splittings differ considerably from what is expected from a Fermi liquidlike orbital picture. In particular, the ground state spin S can change and the excitation
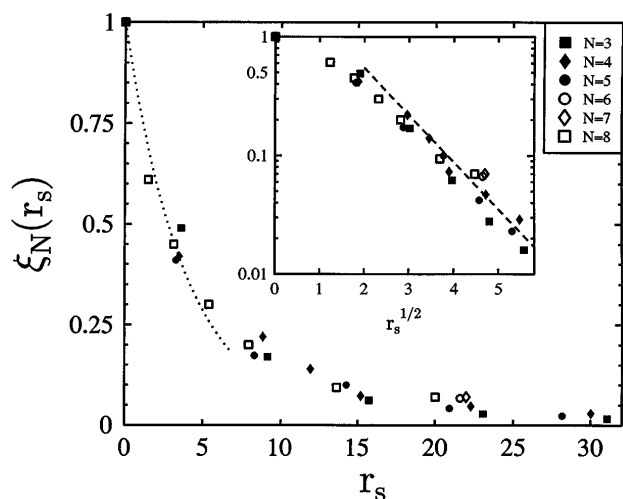
energy of higher-spin states becomes much smaller than $\hbar\omega_0$. This level structure reflects the onset of shell formation in real space. In fact, our large-r_s data in Table I can be rationalized by starting from crystallized electrons located at positions fixed by electrostatics, and then evaluating the quantum corrections due to particle exchange processes, namely, rotation and tunneling. Generalizing the method of Ref. [15] by using semiclassical estimates and group theory to satisfy the Pauli principle, detailed predictions for low-energy spectra can be made in terms of such a *Wigner molecule*. While a detailed discussion of the Wigner molecule will be given elsewhere, it is already apparent from our previous discussion that the value for r_s where the ground state spin changes is not given by $r_c \approx 4$ but is typically larger. Therefore such transitions should be amenable to the Wigner molecule concept, which is indeed the case.

The preceding findings for the energy imply several novel and nontrivial consequences for transport experiments made by weakly coupling the dot to electrodes. In particular, the addition energies following from Table I determine the positions of the conductance peaks measured experimentally by capacitance spectroscopy [1] or by linear transport [2]. Furthermore, high spins occurring close to the ground state energy can lead to negative differential conductances in transport measurements, or even to the disappearance of a conductance peak at low temperatures

TABLE I. MLB data for the energy for various $\{N, S, \lambda\}$ parameter sets. Bracketed numbers denote statistical errors.

| N	S	λ	$E/\hbar\omega_0$	N	S	λ	$E/\hbar\omega_0$
3	3/2	2	8.37(1)	5	5/2	8	42.86(4)
3	1/2	2	8.02(1)	5	3/2	8	42.82(2)
3	3/2	4	11.05(1)	5	1/2	8	42.75(2)
3	1/2	4	10.98(1)	5	5/2	10	48.79(2)
3	3/2	6	13.43(1)	5	3/2	10	48.78(3)
3	3/2	8	15.59(1)	5	1/2	10	48.76(2)
3	3/2	10	17.60(1)	6	3	8	60.42(2)
4	2	2	14.30(5)	6	1	8	60.37(2)
4	1	2	13.414(8)	7	7/2	8	80.59(4)
4	2	4	19.42(1)	7	5/2	8	80.45(4)
4	1	4	18.941(8)	8	4	2	48.3(2)
4	2	6	23.790(12)	8	3	2	47.5(4)
4	1	6	23.624(8)	8	2	2	45.8(3)
4	2	8	27.823(11)	8	1	2	45.6(3)
4	1	8	27.714(8)	8	4	4	69.2(1)
4	2	10	31.538(12)	8	3	4	67.6(3)
4	1	10	31.476(5)	8	2	4	67.3(3)
5	5/2	2	21.29(6)	8	1	4	67.4(3)
5	3/2	2	20.5(1)	8	4	6	86.92(6)
5	1/2	2	20.02(4)	8	3	6	86.82(5)
5	5/2	4	29.12(6)	8	2	6	86.74(4)
5	3/2	4	28.96(4)	8	1	6	86.69(3)
5	1/2	4	28.81(3)	8	4	8	103.26(5)
5	5/2	6	36.44(3)	8	3	8	103.19(4)
5	3/2	6	36.34(2)	8	2	8	103.08(4)
5	1/2	6	36.21(2)				

FIG. 2. Numerical results for $\xi_N(r_s)$. Statistical errors are of the order of the symbol size. The dotted curve, given by $\exp(-r_s/r_c)$ with $r_c = 4$, is a guide to the eye only. The inset shows the same data on a semilogarithmic scale as a function of $\sqrt{r_s}$. The dashed line is given by Eq. (4).

(spin blockade) [16]. According to Table I, $N = 6$ would be a possible candidate in which to find negative differential conductances for the transition to $N = 5$ for $r_s \gtrsim 15$, corresponding to $\hbar\omega_0 \lesssim 0.4$ meV in a GaAs-based quantum dot. Furthermore, the spin-polarized ground state for $N = 3$ at $\lambda \gtrsim 5$ implies that the direct transition into the $S = 0$ ground state for $N = 2$ is spin forbidden. The corresponding conductance peak should then disappear for $\hbar\omega_0 \lesssim 0.5$ meV. A similar situation arises for the $N = 7$ to $N = 6$ transition at $\hbar\omega_0 \lesssim 0.4$ meV. Such phenomena cannot occur in the weakly interacting regime $r_s < r_c$, where entering or escaping electrons are accommodated in effective single-particle orbitals together with their spins. We note that sufficiently large quantum dots allowing for experimental studies of the Wigner molecule phase are within reach of current technology [17].

To conclude, we have presented numerically exact QMC results for parabolic quantum dots covering the full crossover from weak ($r_s \rightarrow 0$) to strong ($r_s \rightarrow \infty$) correlations. The turnover from Fermi liquid to Wigner molecule-like behavior is basically independent of the particle number and characterized by an astonishingly small crossover scale, $r_c \approx 4$. Energy spectra in the low-density regime $r_s > r_c$ differ from single-particle expectations but can be described within a Wigner molecule approach. Detailed predictions have been made for this Wigner molecule phase, which should be directly accessible to current experiments. It is straightforward (and left to future MLB studies) to study other confinements or interaction potentials, or to include a magnetic field.

[1] R. C. Ashoori, Nature (London) **379**, 413 (1996).

[2] L. P. Kouwenhoven *et al.,* in *Mesoscopic Electron Transport,* edited by L. L. Sohn, L. P. Kouwenhoven, and G. Schön, NATO ASI, Ser. E, Vol. 345 (Kluwer Academic Publishers, Dordrecht, 1997).

[3] F. Bolton and U. Rössler, Superlattices Microstruct. **13**, 139 (1993); V. M. Bedanov and F. M. Peeters, Phys. Rev. B **49**, 2667 (1994).

[4] V. Fock, Z. Phys. **47**, 446 (1928); C. G. Darwin, Proc. Cambridge Philos. Soc. **27**, 86 (1930).

[5] U. Merkt, J. Huser, and M. Wagner, Phys. Rev. B **43**, 7320 (1991). See also P. A. Maksym, Phys. Rev. B **53**, 10 871 (1996).

[6] D. Pfannkuche, V. Gudmundsson, and P. A. Maksym, Phys. Rev. B **47**, 2244 (1993).

[7] M. Stopa, Phys. Rev. B **54**, 13 767 (1996); M. Koskinen, M. Manninen, and S. M. Reimann, Phys. Rev. Lett. **79**, 1389 (1997).

[8] E. Y. Loh, Jr. *et al.,* Phys. Rev. B **41**, 9301 (1990).

[9] F. Bolton, Phys. Rev. Lett. **73**, 158 (1994). Typically, the resulting energies are $\approx 10\%$ too large; see Ref. [10].

[10] C. H. Mak, R. Egger, and H. Weber-Gottschick, Phys. Rev. Lett. **81**, 4533 (1998).

[11] C. H. Mak and R. Egger, J. Chem. Phys. **110**, 12 (1999).

[12] The classical point-charge model gives $r_s^3 = C_N \lambda^4$ with $C_N = 4\sin^2(\pi/N)[1 + \delta_{N,4}/\sqrt{8} + \delta_{N,5}/2\cos(\pi/5)]$ for $N = 3, 4, 5$.

[13] B. Tanatar and D. M. Ceperley, Phys. Rev. B **39**, 5005 (1989).

[14] S. T. Chui and B. Tanatar, Phys. Rev. Lett. **74**, 458 (1995).

[15] W. Häusler, Z. Phys. B **99**, 551 (1995).

[16] D. Weinmann, W. Häusler, and B. Kramer, Phys. Rev. Lett. **74**, 984 (1995).

[17] R. C. Ashoori *et al.,* Phys. Rev. Lett. **68**, 3088 (1992).